Community Referee #1

Overall evaluation:

This paper investigates how soil moisture data assimilation can be improved by synergistically combining multi-frequency satellite observations. The authors assimilate soil moisture retrievals from SMAP (L-band), ASCAT (C-band), and FY-3DMWRI (X-band) into the Common Land Model (CoLM) using a Simplified Extended Kalman Filter (SEKF). Overall, the paper provides a meaningful contribution by shifting multi-sensor assimilation from a data-volume-driven approach toward a complementarity- and vegetation-aware strategy. Well fitted and written for publication.

Response:

We sincerely thank you for your valuable time and professional guidance. Your comments have greatly improved the quality of this manuscript.

Following your suggestions, we have conducted a revision of the manuscript, including methodology description, figure presentation, language expression, and discussion depth among other aspects. Regarding your question about seasonal applicability, we extended the period of the assimilation experiment from a single summer to the full year of four seasons (Spring, Summer, Autumn, Winter), thereby verifying the applicability of the vegetation-adaptive assimilation scheme under different seasons. Additionally, we supplemented the details of the source and processing of vegetation type data, improved the readability of the figures by increasing font size and simplifying legends, and discussed the importance of Leaf Area Index (LAI) for future work in the discussion section. Meanwhile, we have corrected existing spelling errors in the text and conducted language proofreading for the full text.

Below, we provide a detailed point-by-point response to your comments, and the corresponding revisions in the manuscript have been highlighted in a specific color.

Comments:

1. The vegetation types used in Figures 5-7 are central to the paper's conclusions. Adding a brief description of how these vegetation classes are defined (e.g. source dataset and thresholds) would improve clarity for readers not familiar with the

classification scheme.

Response:

Thanks for your suggestions. Following your suggestions, we have added a description of vegetation types at line 425 of the revised manuscript. In addition, a spatial distribution map of vegetation cover has been included as Figure 3e to better illustrate the vegetation conditions across the study area. The specific content is as follows:

"The vegetation type data used in this study are derived from the built-in dataset of the CoLM. Considering that each model grid cell typically contains multiple vegetation types, we select the vegetation type with the largest area fraction within each grid cell as the representative vegetation type."

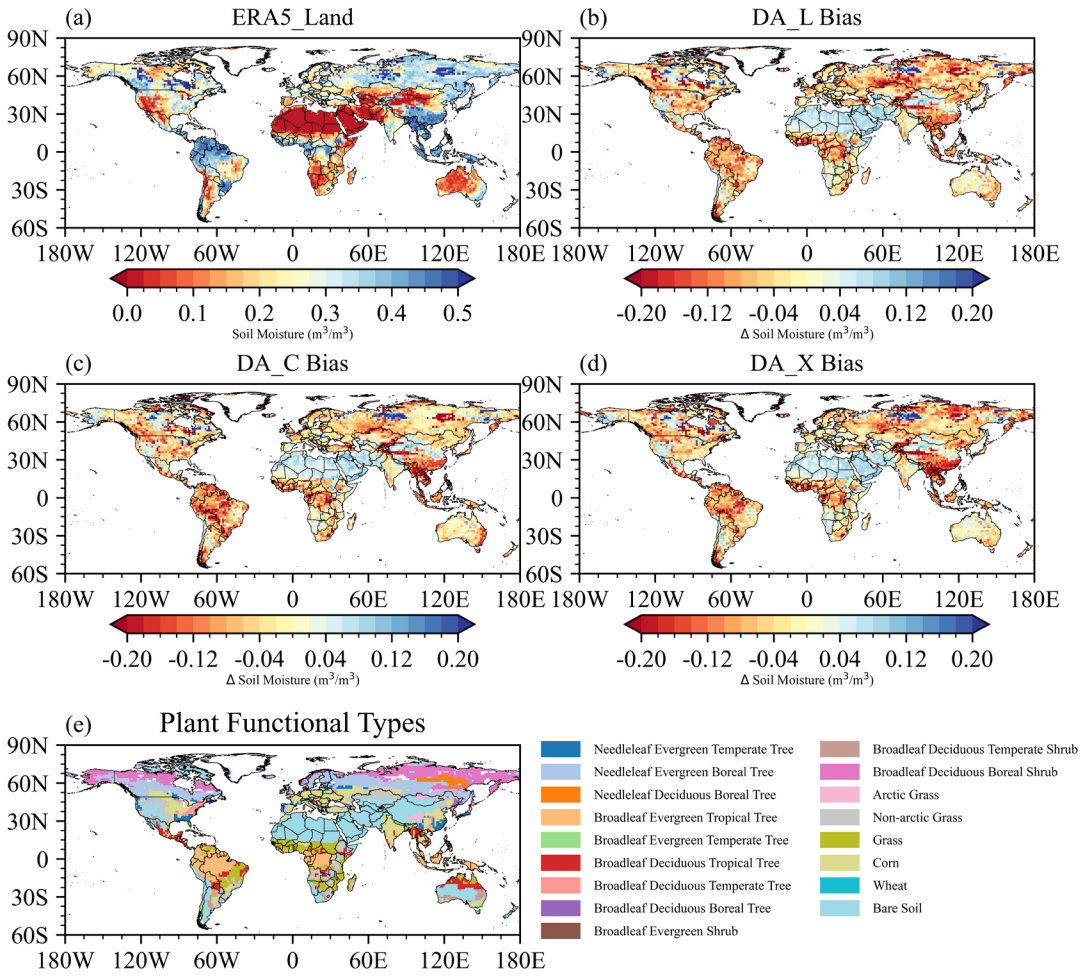

Figure R1: Spatial distribution of mean soil moisture in the top layer (0-7 cm) during 2 June to 3 July 2022. (a) shows the soil moisture from the ERA5_Land product. (b)–(d) show the soil moisture differences of the analysis fields from the DA_L, DA_C, and DA_X assimilation experiments relative to ERA5_Land, respectively (i.e., DA experiment minus ERA5-Land). (e)

shows the spatial distribution of vegetation cover.

2. Some figures (e.g. Figures 5,6, and 9) contain many panels and colors, which makes interpretation difficult. Increasing font sizes and simplifying legends would enhance readability.

Response:

Thanks for your suggestions. Following your suggestions, we have increased the font size and simplified the legends in Figures 5, 6, and 9. The revised figures are shown as Figures R2, R3, and R4.

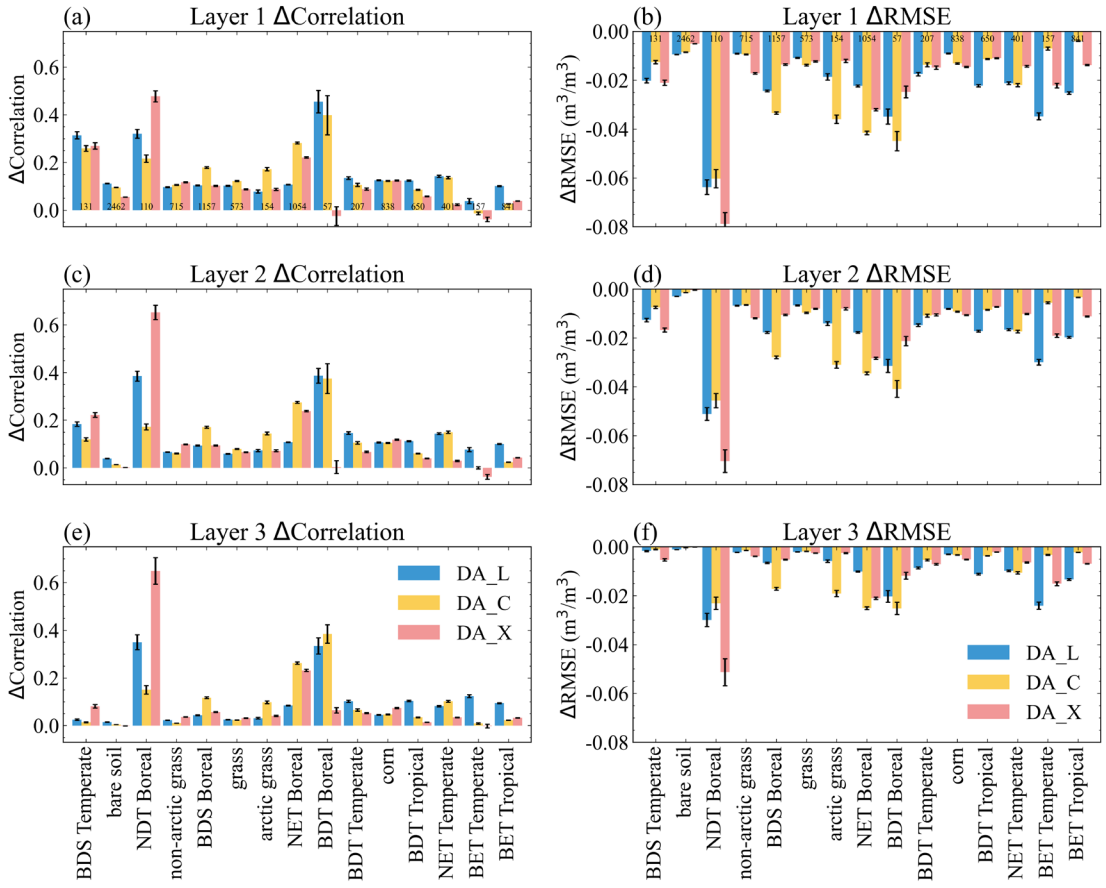

Figure R2: Changes in correlation coefficient (left panels; after-minus-before assimilation) and RMSE (right panels; after-minus-before assimilation) of soil moisture relative to ERA5-Land during 2 June to 3 July 2022, shown as a function of vegetation type. (a, c, e) is correlation coefficients for layer 1, layer 2, and layer 3, respectively, and (b, d, f) is the corresponding RMSE for layer 1, layer 2, and layer 3, respectively. Error bars denote 95% confidence intervals, and numbers below represent the sample size, which is identical across all groups.

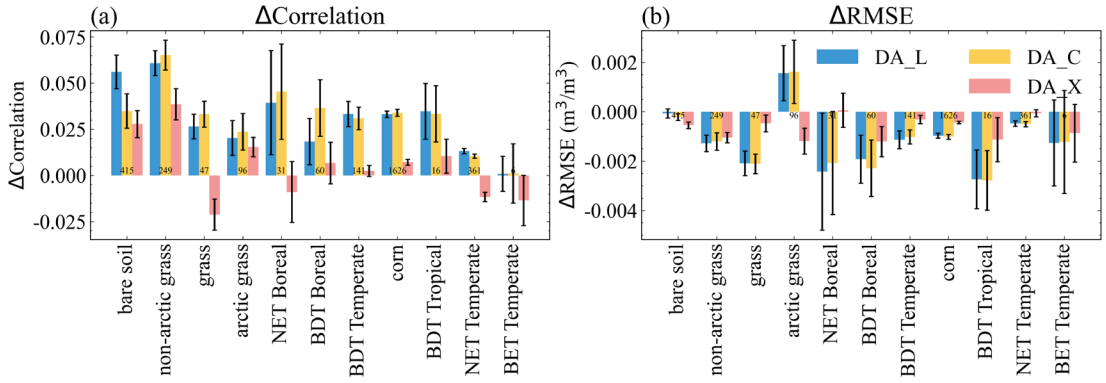

Figure R3: Same as Figure 5, but for comparison between model soil moisture and in situ observations at 0–10 cm depth. (a) is correlation coefficients for 0-l0 cm, and (b) is the corresponding RMSE for 0-10 cm. Error bars denote 95% confidence intervals, and numbers below represent the sample size, which is identical across all groups.

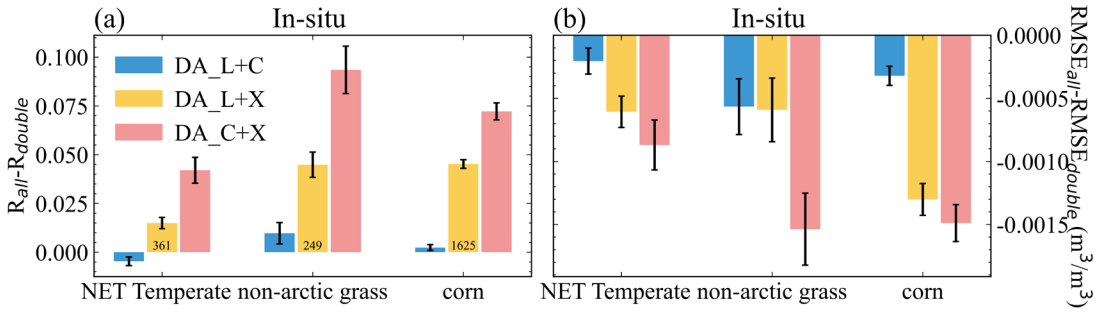

Figure R4: Changes in correlation coefficient (a) and RMSE (b) between model output and in situ observations after adding a third satellite product to each two-product assimilation combination, shown for selected vegetation types. Error bars denote 95% confidence intervals, and numbers below represent the sample size, which is identical across all groups.

3. A small number of grammatical issues remain (e.g., "improving the shill of the CoLM" in Section 3.4). A final round of language proofreading would further improve the manuscript's presentation quality.

Response:

Thanks for your suggestions. Following your suggestions, we corrected the spelling error in Section 3.4 by replacing “shill” with “skill”. We also proofread the manuscript and corrected grammatical, spelling, and punctuation issues throughout the text.

4. The experiments are conducted over a relatively short period (June-August 2022).

While the results are convincing for summer conditions, soil moisture dynamics and microwave retrieval performance can vary substantially across seasons (e.g., frozen soils, snow cover, phenological changes), This limitation raises questions about the generalizability of the proposed vegetation-adaptive scheme, Extending the analysis to additional seasons or providing a clearer discussion of this limitation would strengthen the conclusions.

Response:

Thank you for your suggestions. Following your suggestions, we have extended the assimilation experiments to cover all four seasons of the year (Spring MAM, Summer JJA, Autumn SON, and Winter DJF). Results from other seasons also support our conclusion. The key to achieving positive results with X-band lies in selecting X-band products with smaller observational errors. Indeed, as the reviewer pointed out, seasonal variations affect the selection of X-band data. Through the comparative analysis of multi-season assimilation performance, we found that, in addition to vegetation type, the seasonal variation of vegetation should also be considered when assessing the impact of X-band assimilation.

We have added the relevant analysis to Figures 18 and 19 in Lines 722-766 of the revised manuscript, where Figure 18 shows the seasonal assimilation performance for representative vegetation types and Figure 19 presents the seasonal probability density distributions of the correlation coefficient differences among different assimilation experiments. The revised text is as follows:

To further investigate the differences in assimilation results across seasons, we extended the experiments to include spring (MAM), autumn (SON), and winter (DJF). Figure R5 presents a comparison of the correlation coefficients between the DA_L+C and DA_ALL experiments across the four seasons for different vegetation types. The Non-arctic Grass and Corn regions exhibit more pronounced seasonal differences. In summer (JJA) and winter (DJF), the growth of grasses and crops tends to stabilize, or the vegetation density decreases significantly. As a result, observation errors are relatively stable, making the addition of the X-band more likely to result in positive effects. As shown in the figure, the orange bars are noticeably higher than the blue bars

during summer and winter.

Conversely, during the transitional phases of spring (MAM) and autumn (SON), the orange bars are lower than the blue bars, indicating that the inclusion of X-band data degrades the overall assimilation performance. This is likely because vegetation undergoes rapid growth or senescence during spring and autumn, accompanied by drastic changes in morphological structure and water content. As a result, X-band observations, which are more sensitive to vegetation effects, are more strongly influenced under these conditions. When vegetation dynamics are not adequately represented, soil moisture retrievals may exhibit increased variability and occasional anomalous estimates, thereby increasing observation errors (Dash and Sinha, 2019; Stradiotti et al., 2025). This elevated error uncertainty causes the assimilation of X-band data to be prone to negative impacts.

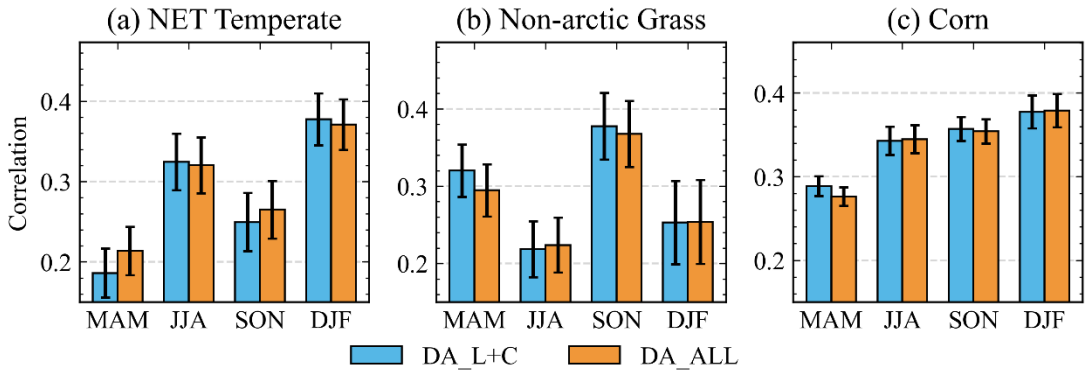

Figure R5: Comparison of assimilation performance for representative vegetation types across different seasons. The figure shows the correlation coefficients between simulated soil moisture and station observations for (a) NET Temperate, (b) Non-arctic Grass, and (c) Corn across the four seasons. The blue and orange bars represent the DA_L+C and DA_ALL experiments, respectively. Error bars indicate the 95% confidence intervals.

Based on the above analysis, the winter settings follow those of summer, where X-band data is excluded only in dense vegetation areas. In spring and autumn, X-band data is not introduced in Corn and Non-arctic Grass. This is because Cron and Non-arctic Grass are undergoing rapid growth or senescence during the transitional phases of spring and autumn. The resulting substantial changes in vegetation morphology and water content are prone to enhancing X-band scattering noise and increasing observation uncertainty.

Figure R6 displays the PDF of the differences in correlation coefficients between the three sets of assimilation experiments and the control experiment based on in situ observations. As shown in Figure R6, the differences for all assimilation experiments are primarily distributed in the range greater than zero, indicating that assimilating satellite data produces a positive effect. The probability distribution of these differences reveals that improvements are more likely to occur during spring and autumn, where the probability of a correlation coefficient increment exceeding 0.5 is higher than in the other two seasons. In contrast, the assimilation improvement in winter is relatively small, with the magnitude of correlation coefficient increments mainly concentrated around 0.1.

Comparing the improvement effects of different assimilation experiments, it is evident that the DA_NEW experiment reduces the probability of negative effects across all seasons, shifting the overall probability density distribution toward the positive effect interval. Compared with the DA_ALL experiment, the improvements of the new scheme in spring, summer, and autumn are more concentrated around 0.3, while in winter, they are concentrated around 0.1. Furthermore, the mean correlation coefficients for each season indicate that the DA_NEW experiment produces higher average values than both the DA_L+C and DA_ALL experiments in every season. This demonstrates that the new scheme, by dynamically adjusting the combination of multi-source data, better integrates the advantages of multi-source observations, thereby improving global land surface assimilation performance.

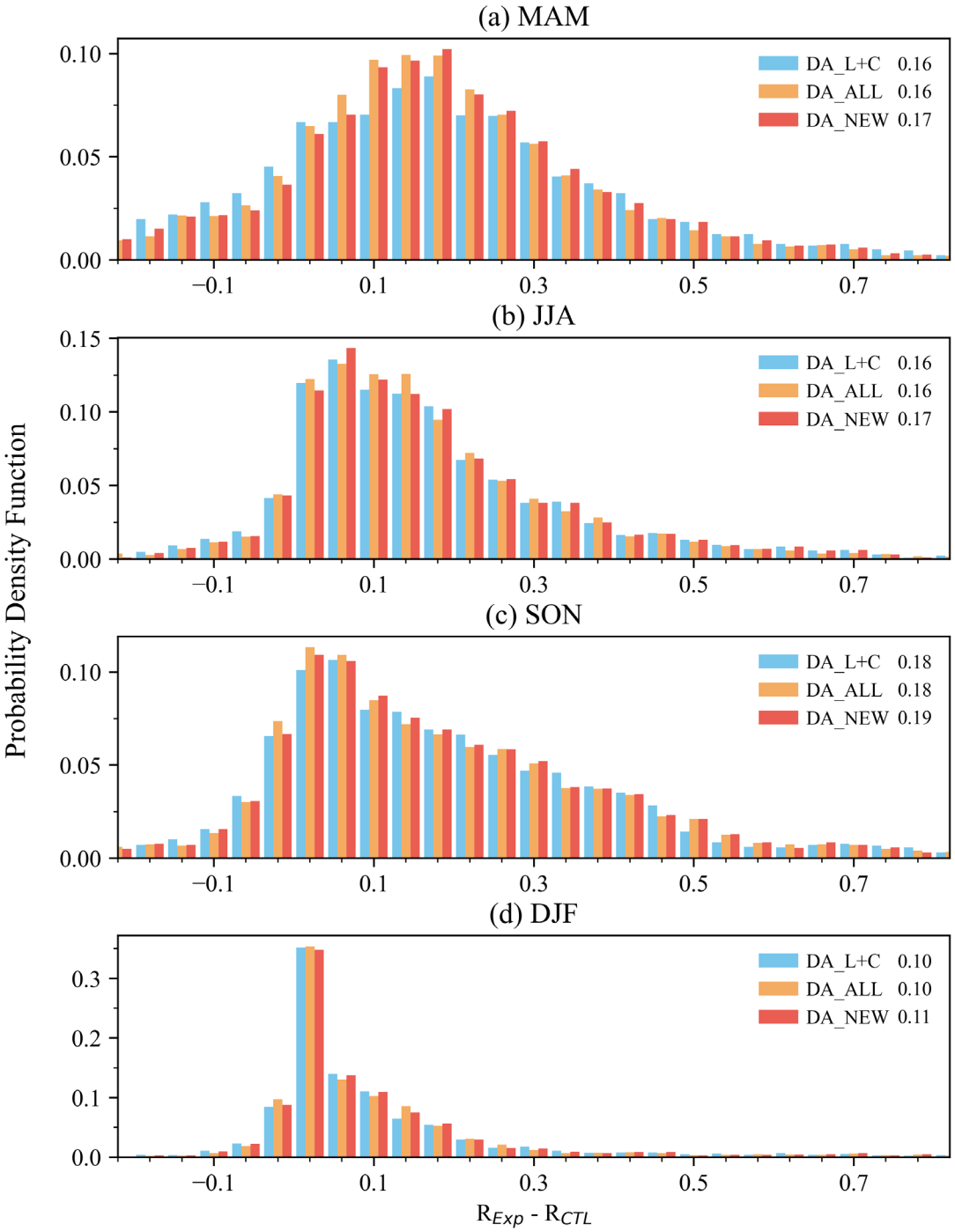

Figure R6: Seasonal variations in the probability density functions of the correlation coefficient differences between the assimilation experiments (DA_L+C, DA_ALL, and DA_NEW) and the control experiment based on station observations. (a) Spring (MAM), (b) Summer (JJA), (c) Autumn (SON), and (d) Winter (DJF). The numbers in the upper-right corner indicate the mean values.

Furthermore, regarding the frozen soil and snow-covered scenarios you mentioned, the soil dielectric constant undergoes fundamental changes under these conditions. Consequently, the physical relationship between microwave signals and liquid soil

moisture ceases to hold. For this reason, existing passive microwave soil moisture products flag the corresponding pixels as missing values during periods of frozen soil and snow cover, providing no soil moisture retrieval results. As a result, the assimilation system does not receive any satellite observation inputs over these areas.

The following references have been added to the reference part of the revised manuscript:

Dash, S. K. and Sinha, R.: A Comprehensive Evaluation of Gridded L-, C-, and X-Band Microwave Soil Moisture Product over the CZO in the Central Ganga Plains, India, Remote Sensing, 14, 1629, https://doi.org/10.3390/rs14071629, 2019.

Stradiotti, P., Gruber, A., Preimesberger, W., and Dorigo, W.: Accounting for seasonal retrieval errors in the merging of multi-sensor satellite soil moisture products, Science of Remote Sensing, 12, 100242, https://doi.org/10.1016/j.srs.2025.100242, 2025.

5. I strongly suggest that the authors acknowledge related studies that "assimilation of Sentinel-derived leaf area index to improve the representation of surface-groundwater interactions in irrigation districts." Citing and briefly discussing such work would strengthen the linkage between the proposed framework and existing literature, and help position the study within the broader context of land data assimilation research.

Response:

Thanks for your suggestions. Following your suggestions, we added a discussion of the assimilation effects of different retrieval products and further connected our multi-frequency assimilation optimization scheme with previous research. The added discussion can be found in Lines 805–808 of the revised manuscript, as follows:

"Additionally, directly assimilating vegetation state variables offers another promising pathway beyond using vegetation solely for sensor selection (Albergel et al., 2019; Zafarmomen et al., 2024; Xu et al., 2025). For instance, Zafarmomen et al. (2024) showed that assimilating Sentinel-derived leaf area index improves surface-groundwater interaction representation, suggesting that joint assimilation of soil moisture and vegetation indices could better constrain complex hydrological processes."

The following references have been added to the reference part of the revised manuscript:

Albergel, C., Dutra, E., Bonan, B., Zheng, Y., Munier, S., Balsamo, G., de Rosnay, P., Muñoz-Sabater, J., and Calvet, J.-C.: Monitoring and Forecasting the Impact of the 2018 Summer Heatwave on Vegetation, Remote Sensing, 11, 520, https://doi.org/10.3390/rs11050520, 2019.

Xu, Y., Calvet, J.-C., and Bonan, B.: The joint assimilation of satellite observed LAI and soil moisture for the global root zone soil moisture production and its impact on land surf ace and ecosystem variables, Agric. For. Meteorol., 360, 110299, https://doi.org/10.1016/j.ag rformet.2024.110299, 2025.

Zafarmomen, N., Alizadeh, H., Bayat, M., Ehtiat, M., and Moradkhani, H.: Assimilation of sentinel-based leaf area index for modeling surface-ground water interactions in irrigation districts, Water Resour. Res., 60, e2023WR036080, https://doi.org/10.1029/2023WR036080, 2024.